Abstract ID: 92

Advancing FAPI Theranostics: Preclinical evaluation of [^{177}Lu]Lu-DOTAGA.Glu.(FAPI)$_2$ and [^{177}Lu]Lu-DO3A.Glu.(FAPI)$_2$ with human dosimetry extrapolation to 177-lutetium and 161-terbium

Adrianna Bilinska[1], Naveen Kumar[1], Silvano Gnesin[2], Tilman Läppchen[1], Elena Menéndez[1], Marcel Martin[3], Frank Rösch[3], Axel Rominger[1], Eleni Gourni[1]

[1]Department of Nuclear Medicine, Inselspital, Bern University Hospital, Switzerland,

[2]Institute of Radiation Physics, Lausanne University Hospital, Lausanne, Switzerland

[3]Department of Chemistry–TRIGA site, Johannes Gutenberg-University Mainz, Germany

Introduction

The development of FAPI-based radiopharmaceuticals has gained significant interest due to extreme potential to target multiple tumor types. ^{177}Lu-labeled FAPI agents are under active investigation, while ^{161}Tb offers potential advantages through the emission of conversion and Auger electrons.
This study provides the first comparative *in vivo* evaluation of two ^{177}Lu-labeled FAPI dimers, DOTAGA.Glu.(FAPI)$_2$ and DO3A.Glu.(FAPI)$_2$, with human dosimetry extrapolation supporting future application of both ^{177}Lu and ^{161}Tb in targeted radionuclide therapy.

Materials and methods

DOTAGA.Glu.(FAPi)$_2$ and DO3A.Glu.(FAPi)$_2$ were labeled with lutetium-177. Both dimers were evaluated *in vivo* (biodistribution, metabolic stability, SPECT/CT imaging and dosimetry) on PC3 xenografts. Furthermore, extrapolation of the murine dosimetry data to human estimates was performed for [^{177}Lu]Lu-DOTAGA.Glu.(FAPI)$_2$, [^{177}Lu]Lu-DO3A.Glu.(FAPI)$_2$, [^{161}Tb]Tb-DOTAGA.Glu.(FAPI)$_2$ and [^{161}Tb]Tb-DO3A.Glu.(FAPI)$_2$.

Results

Radiolabeling

DOTAGA.Glu.(FAPI)$_2$ and DO3A.Glu.(FAPI)$_2$ (Fig. 1) were labelled with lutetium-177 at > 98% radiochemical purity, with apparent molar activity (A_m) of 6–38 GBq/µmol, depending on the study. No colloid formation was observed. The formulated ^{177}Lu-labeled FAPI radioligands remained highly stable, with no radiolysis or chemical decomposition observed up to 96 h post-labeling, respectively.

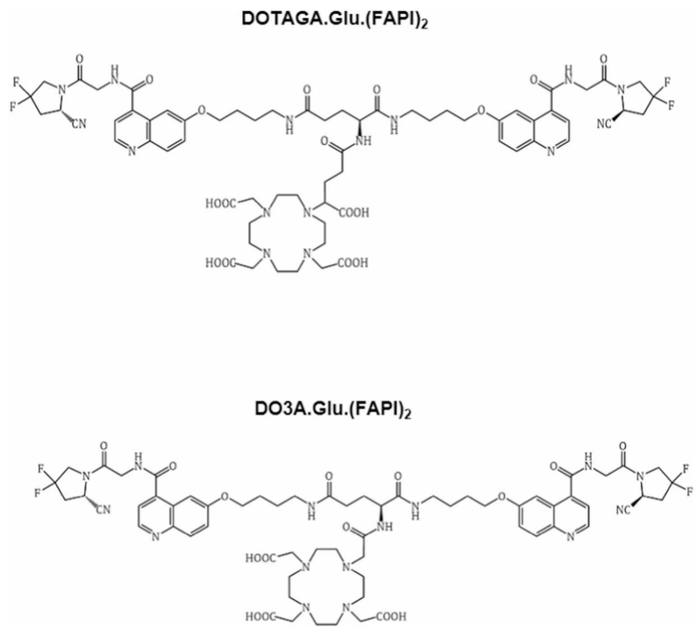

Figure 1. Schematic representations of DOTAGA.Glu.(FAPI)$_2$ and DO3A.Glu.(FAPI)$_2$

Biodistribution studies

Biodistribution data of PC3-mice are shown in Fig. 2A and B. [^{177}Lu]Lu-DOTAGA.Glu.(FAPI)$_2$ and [^{177}Lu]Lu-DO3A.Glu.(FAPI)$_2$ showed ~15%I.A./g tumor uptake at 4 h p.i., dropping by ~50% at 24 h. At 48 h, [^{177}Lu]Lu-DOTAGA.Glu.(FAPI)$_2$ had significantly higher tumor uptake (5.1 ± 0.1%I.A./g) than [^{177}Lu]Lu-DO3A.Glu.(FAPI)$_2$ (3.1 ± 0.5%I.A./g; $p < 0.0001$), and remained higher even at 96 h (2.2 ± 0.2 vs. 1.0 ± 0.03%I.A./g; $p < 0.001$). Both showed low background and blood activity (~2%I.A./g) at 4 h. Elevated uptake in salivary glands and bone was observed. Clearance from tumor, salivary glands, and bone was similar in both cases.

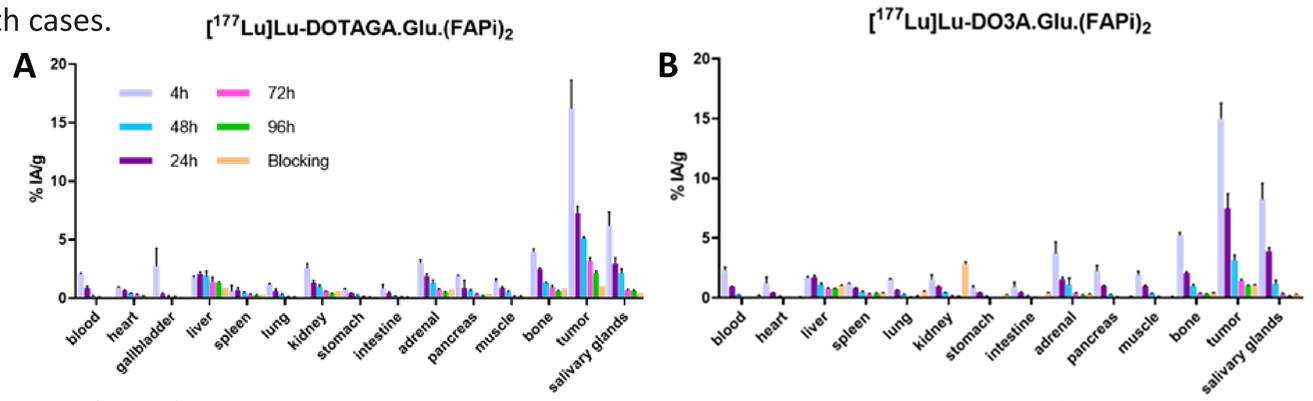

Figure 2. Biodistribution data of (A) [^{177}Lu]Lu-DOTAGA.Glu.(FAPI)$_2$ and (B) [^{177}Lu]Lu-DO3A.Glu.(FAPI)$_2$ at 4, 24, 48, 72 and 96 h p.i. with blocking at 4 h p.i. in PC3-mice.

SPECT/CT imaging

SPECT/CT images (Fig. 3) match the biodistribution data, with slightly elevated background at 4 h p.i., particularly in bones and salivary glands. The images clearly demonstrate significant tumor uptake across all time points, with [^{177}Lu]Lu-DO3A.Glu.(FAPI)$_2$ showing faster clearance compared to [^{177}Lu]Lu-DOTAGA.Glu.(FAPI)$_2$, at later time points. The blocking studies confirmed the specific binding of both radioligands.

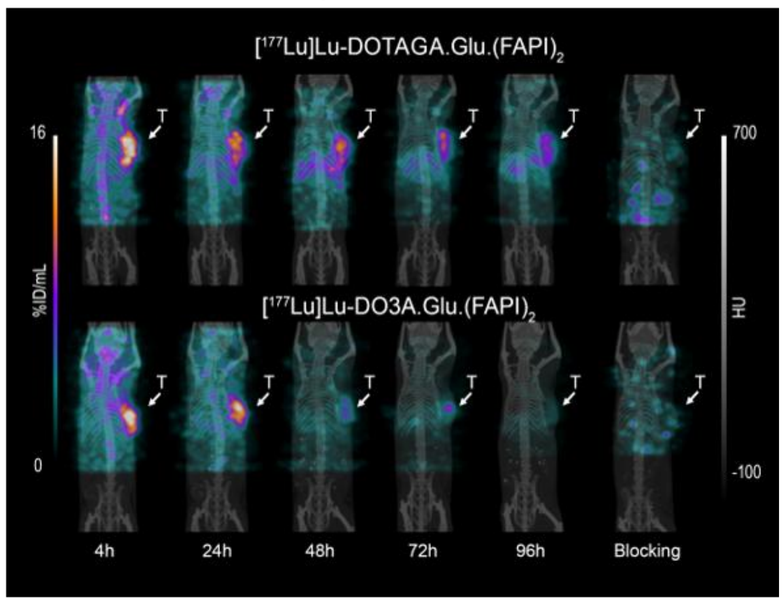

Figure 3. SPECT/CT images of [^{177}Lu]Lu-DOTAGA.Glu.(FAPI)$_2$ and [^{177}Lu]Lu-DO3A.Glu.(FAPI)$_2$ in PC3-mice at 4, 24, 48, 72 and 96 h p.i., with blocking at 4 h p.i.

Metabolic stability

The radio-HPLC analysis of mouse plasma samples at 30 min p.i. showed that the circulating radioactivity consisted exclusively of intact 177Lu-labeled radioligands in both cases (Fig. 4A-B).

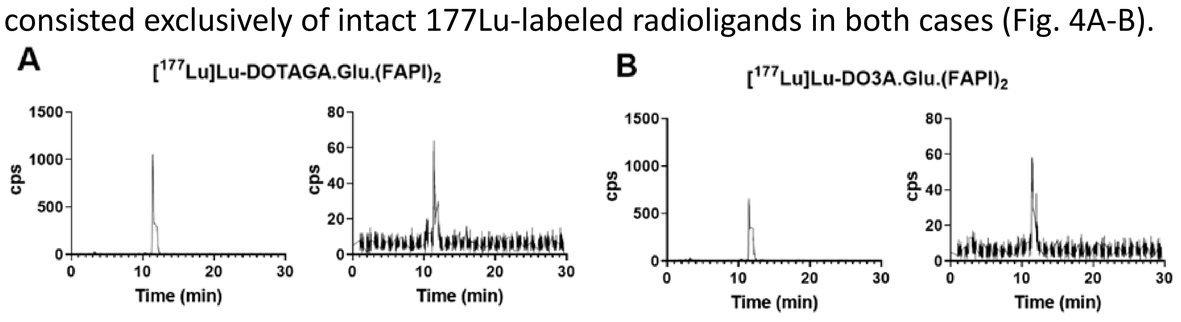

Figure 4. Representative radio-HPLC chromatograms of **(A)** [^{177}Lu]Lu-DOTAGA.Glu.(FAPI)$_2$ and **(B)** [^{177}Lu]Lu-DO3A.Glu.(FAPI)$_2$ before injection (left) and from blood samples at 30 min p.i. (right).

Murine dosimetry

Organ time-activity curves were derived from biodistribution data (4–96 h p.i.) in PC3 tumor-bearing mice and corrected for tumor sink effects. Time-integrated activity coefficients (TIACs) were calculated using bi-exponential fitting. Tumor effective half-life was longer for [^{177}Lu]Lu-DO3A.Glu.(FAPI)$_2$ (≈51 h) compared with [^{177}Lu]Lu-DOTAGA.Glu.(FAPI)$_2$ (≈39 h).[^{177}Lu]Lu-DOTAGA.Glu.(FAPI)$_2$ showed higher retention in non-tumoral organs.

Human dosimetry extrapolation

Murine TIACs were extrapolated to adult human male and female reference phantoms using organ-to-body-mass scaling and implemented in OLINDA/EXM software.
[^{177}Lu]Lu-DOTAGA.Glu.(FAPI)$_2$ resulted in higher absorbed doses (Gy/GBq) across most organs compared with [^{177}Lu]Lu-DO3A.Glu.(FAPI)$_2$. Osteogenic cells and salivary glands received the highest organ doses for both compounds (Tab. 1). Assuming identical biological behavior and similar physical half-lives, human dosimetry was extrapolated from ^{177}Lu to ^{161}Tb.^{161}Tb-labeled radioligands delivered ~38% higher absorbed doses to tissues compared with their ^{177}Lu counterparts (Tab. 2).

Average human absorbed dose extrapolations (mGy/Mbq)

	[^{177}Lu]Lu-DOTAGA.Glu.(FAPI)$_2$		[^{177}Lu]Lu-DO3A.Glu.(FAPI)$_2$	
	M	**F**	**M**	**F**
Kidneys	4.08E-02±0.002	4.97E-02±0.002	2.09E-02±0.001	2.54E-02±0.001
Liver	1.64E-01±0.01	2.00E-01±0.02	6.00E-02±0.002	7.30E-02±0.003
Pancreas	3.11E-02±0.002	3.90E-02±0.002	2.12E-02±0.001	2.62E-02±0.001
Salivary glands	1.03E-01±0.004	1.26E-01±0.004	7.27E-02±0.01	8.81E-02±0.01
Osteogenic Cells	9.26E-02±0.01	8.92E-02±0.01	6.64E-02±0.002	6.24E-02±0.002
Red marrow	2.38E-02±0.002	3.24E-02±0.003	2.43E-02±0.001	3.06E-02±0.001
Spleen	2.87E-02±0.01	3.53E-02±0.01	5.27E-02±0.002	6.42E-02±0.003
Lungs	3.74E-02±0.003	4.59E-02±0.004	3.40E-02±0.01	4.16E-02±0.01
Small intestine	4.17E-02±0.01	5.84E-02±0.02	3.27E-02±0.002	4.29E-02±0.003
Total Body	3.25E-02±0.003	4.42E-02±0.01	2.71E-02±0.001	3.44E-02±0.002

Table 1. Target organ absorbed dose for [^{177}Lu]Lu-DOTAGA.Glu.(FAPI)$_2$ and [^{177}Lu]Lu-DO3A.Glu.(FAPI)$_2$

Average human absorbed dose extrapolations (mGy/Mbq)

	[^{161}Tb]Tb-DOTAGA.Glu.(FAPI)$_2$		[^{161}Tb]Tb-DO3A.Glu.(FAPI)$_2$	
	M	**F**	**M**	**F**
Kidneys	5.60E-02±0.002	6.83E-02±0.003	2.84E-02±0.001	3.48E-02±0.001
Liver	2.29E-01±0.02	2.78E-01±0.02	8.31E-02±0.003	1.01E-01±0.004
Pancreas	4.25E-02±0.002	5.34E-02±0.003	2.88E-02±0.001	3.59E-02±0.001
Salivary glands	1.43E-01±0.01	1.73E-01±0.01	1.00E-01±0.01	1.22E-01±0.01
Osteogenic Cells	1.24E-01±0.01	1.23E-01±0.01	8.97E-02±0.003	8.70E-02±0.003
Red marrow	3.37E-02±0.003	4.59E-02±0.01	3.45E-02±0.001	4.37E-02±0.002
Spleen	3.92E-02±0.01	4.83E-02±0.01	7.27E-02±0.003	8.87E-02±0.004
Lungs	5.19E-02±0.004	6.37E-02±0.01	4.73E-02±0.01	5.78E-02±0.01
Small intestine	5.69E-02±0.02	4.17E-02±0.01	2.85E-02±0.001	3.72E-02±0.002
Total Body	4.51E-02±0.01	6.01E-02±0.01	3.70E-02±0.002	4.70E-02±0.002

Table 2. Target organ absorbed dose extrapolated for [^{161}Tb]Tb-DOTAGA.Glu.(FAPI)$_2$ and [^{161}Tb]Tb-DO3A.Glu.(FAPI)$_2$

Conclusion

Our study provide strong evidence for the potential use of [^{177}Lu]Lu-DOTAGA.Glu.(FAPI)$_2$ and [^{177}Lu]Lu-DO3A.Glu.(FAPI)$_2$ as therapeutic radiotracers for targeting FAP-expressing tumors. Human dosimetry projections for both ^{177}Lu and ^{161}Tb offer valuable insights into the clinical translation of those FAP-targeted radiopharmaceuticals.

OncoProTools
Funded by the European Union
UNIVERSITÄT BERN
INSELSPITAL
UNIVERSITÄTSSPITAL BERN
HÔPITAL UNIVERSITAIRE DE BERNE